Electronic Supplementary Information

A novel lithium-impregnated hollow MOF-based electrolyte realizing an optimum balance between ionic conductivity and the transference number in solid-like batteries

Fencheng Tao, Li Tian, Zixin Liu, Ruixue Cui, Meiying Liu, Xiaomin Kang* and Zhiliang Liu*

College of Chemistry and Chemical Engineering, Inner Mongolia University, Hohhot 010021, P.R. China. E-mail: kangxm@imu.edu.cn and cezlliu@imu.edu.cn; Fax: +86-471-4992261; Tel: +86-471-4992261.

Contents

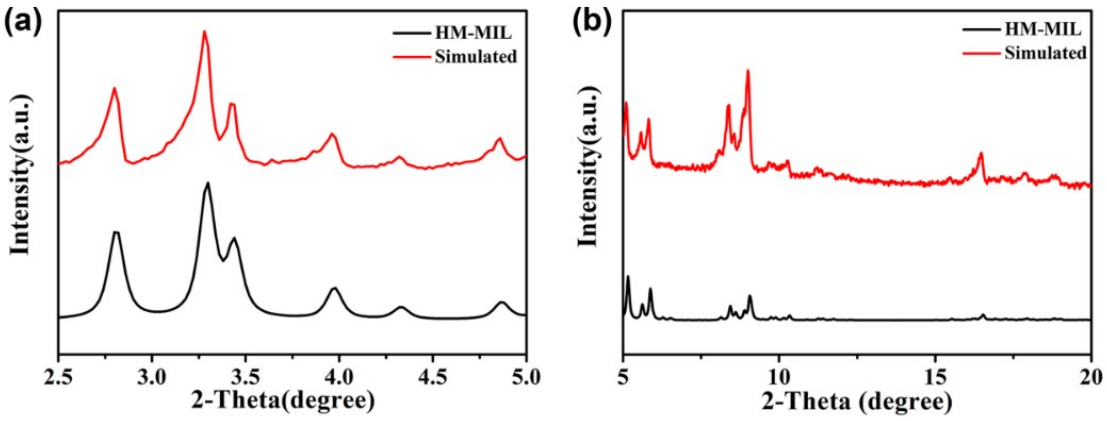

Figure S1. PXRD patterns of the synthesized hollow mesopores HM-MIL match well with that of simulated ones.

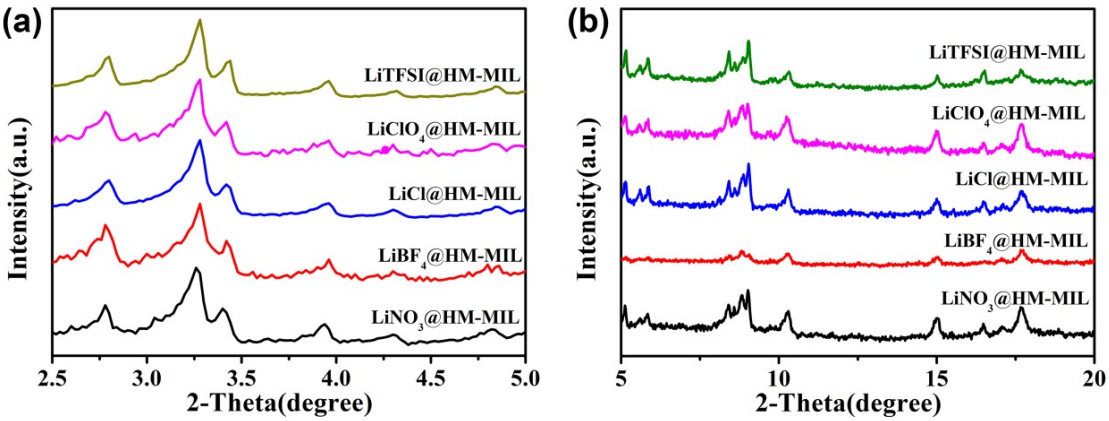

Figure S2. The PXRD patterns of the synthesized $LiNO_3$@HM-MIL, $LiBF_4$@HM-MIL, LiCl@HM-MIL, $LiClO_4$@HM-MIL and LiTFSI@HM-MIL.

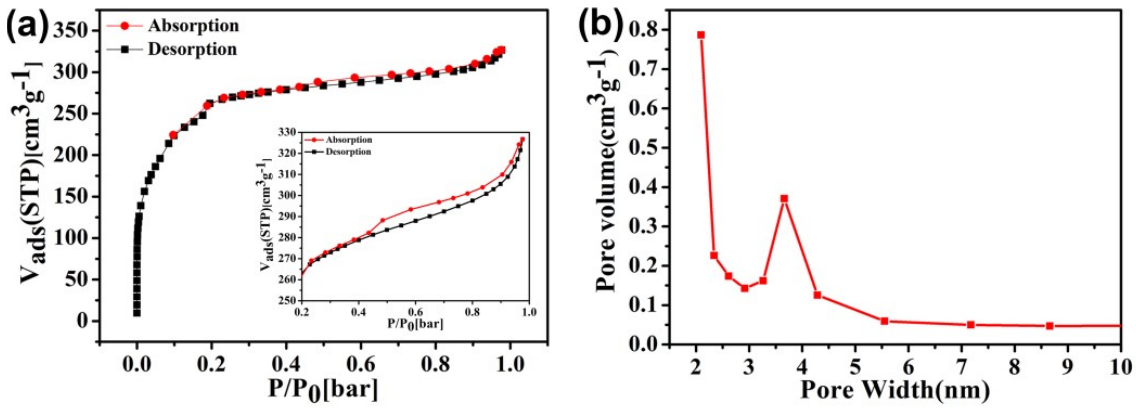

Figure S3. (a) The BET of the synthesized hollow mesoporous HM-MIL; (b) Pore size distribution of the synthesized hollow mesoporous HM-MIL.

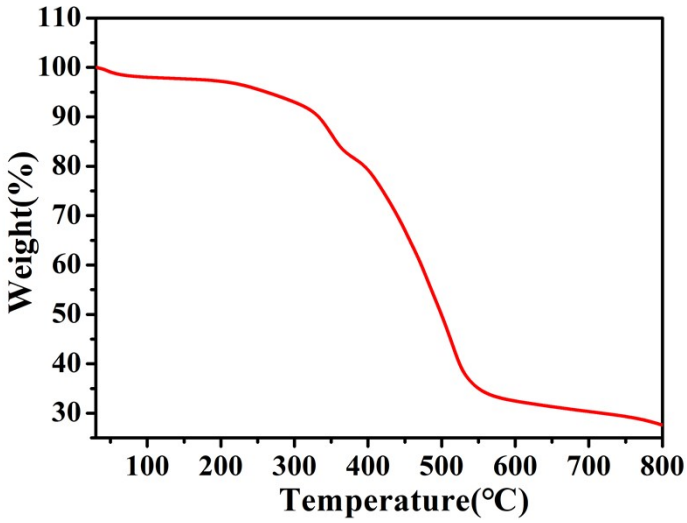

Figure S4. The TGA curves of synthesized hollow mesoporous HM-MIL.

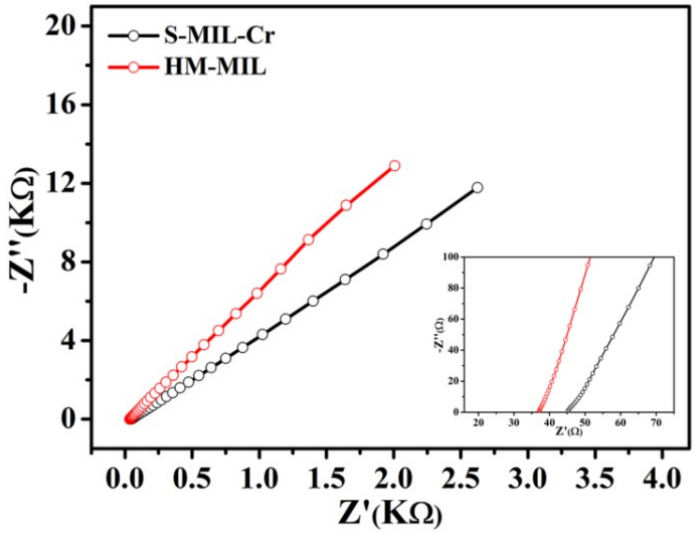

Figure S5. EIS of the S-MIL-Cr electrolyte and hollow mesoporous HM-MIL electrolyte (25 °C), and the internal shows a magnified view of the high frequency area.

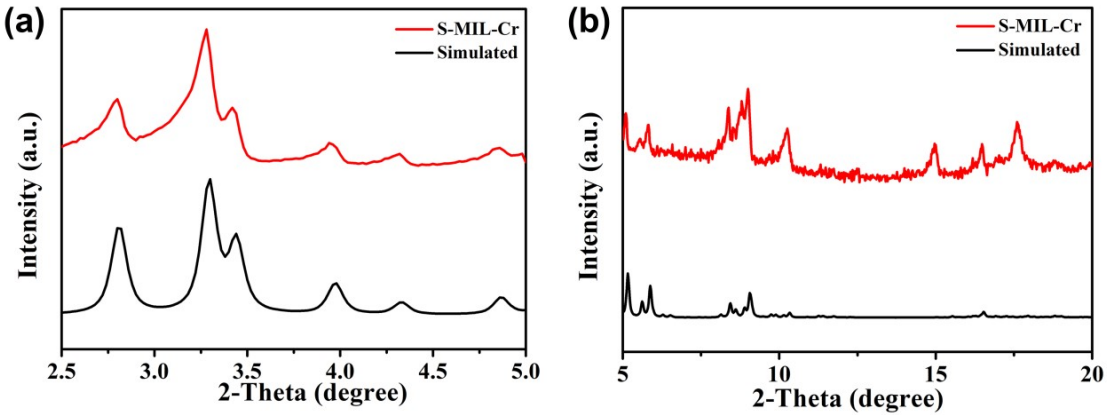

Figure S6. The PXRD patterns of the synthesized solid S-MIL-Cr.

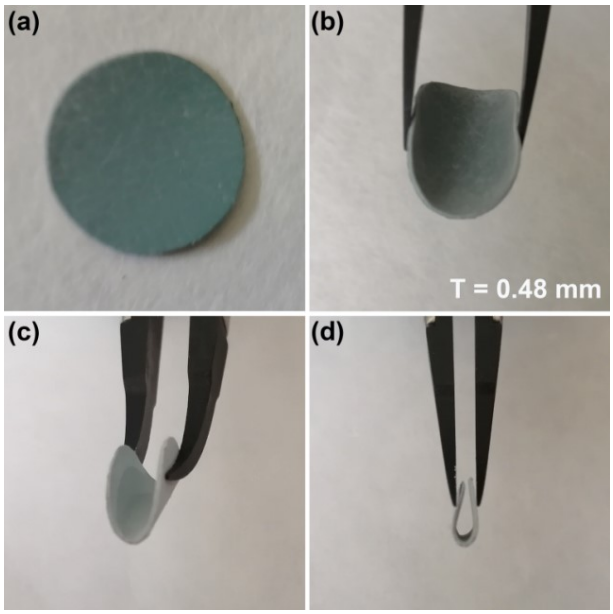

Figure S7. (a) Photograph of the $LiNO_3$@HM-MIL electrolyte membrane; (b-d) Flexible electrolyte membranes of $LiNO_3$@HM-MIL under different bending degrees.

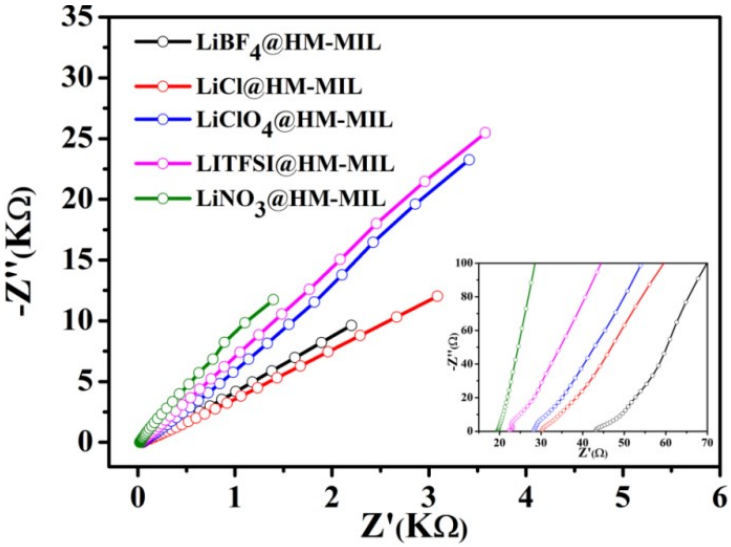

Figure S8. The EIS of the synthesized $LiBF_4$@HM-MIL, LiCl@HM-MIL, $LiClO_4$@HM-MIL, LiTFSI@HM-MIL and $LiBF_4$@HM-MIL at 25 °C (the internal shows a magnified view of the high frequency area).

Table S1. The ionic conductivity and ICP results for HM-MIL after immersing different lithium salt solutions.

NO.	Materials	σ (S cm^{-1})	Lithium content (wt%)
1	$LiNO_3$@HM-MIL	1.24×10^{-3}	12
2	LiTFSI@HM-MIL	9.36×10^{-4}	11.2
3	$LiClO_4$@HM-MIL	7.90×10^{-4}	0.001
4	LiCl@HM-MIL	7.54×10^{-4}	0.013
5	$LiBF_4$@HM-MIL	5.17×10^{-4}	1.01

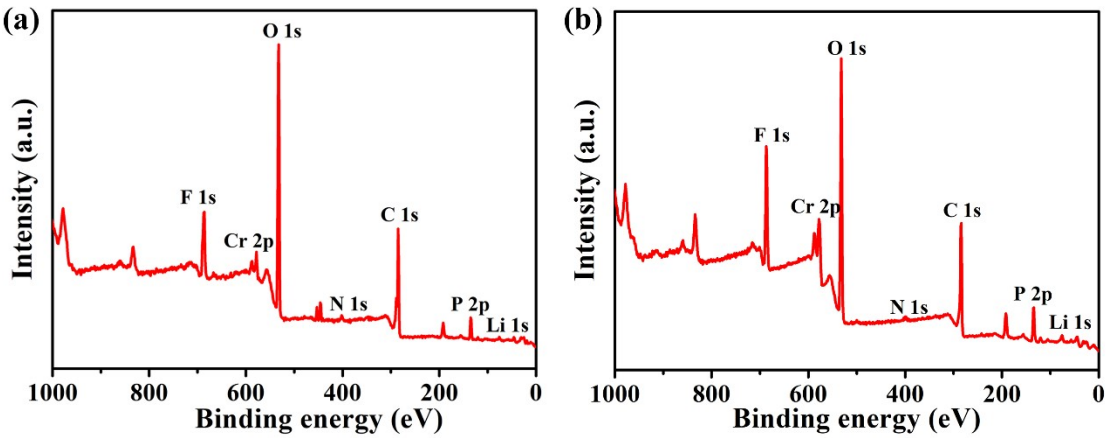

Figure S9. (a) The X-ray photoelectron spectra (XPS) of the $LiNO_3$@HM-MIL after the activation treatment by $LiPF_6$; (b) The XPS of $LiNO_3$@HM-MIL after the treatment of argon etching about one minute.

Table S2. Summary of ionic conductivity for MOFs-based solid-state electrolytes at different temperature ranges.

NO.	Materials	Temperature Range	σ (S cm^{-1})	Ref
1	LGZ	30-80°C	1.61×10^{-4} (30°C) 5.26×10^{-4} (80°C)	S1
2	LCMOF-1/PVDF-HFP/Li-IL	-20-80°C	6.7×10^{-4} (30°C) 5.01×10^{-4} (80°C)	S2
3	UiO-66-LiSS	25-90°C	6.0×10^{-5} (25°C) 7.90×10^{-5} (80°C) 1.10×10^{-4} (90°C)	S3
4	MOF-688	-40-60°C	3.40×10^{-4} (20°C) 4.60×10^{-4} (30°C)	S4
5	UiOLiTFSI	25-70°C	2.07×10^{-4} (25°C) 1.39×10^{-3} (70°C)	S5
6	ZIF-67@ZIF-8	-20-100°C	3.44×10^{-4} (-20°C) 4.98×10^{-3} (100°C)	S6
7	Li-IL@MOF	-20-100°C	2.20×10^{-5} (-20°C) 4.90×10^{-3} (100°C)	S7
8	**$LiNO_3$@HM-MIL**	**20-120°C**	**6.46×10^{-4} (20°C)** **5.06×10^{-3} (120°C)**	**This work**

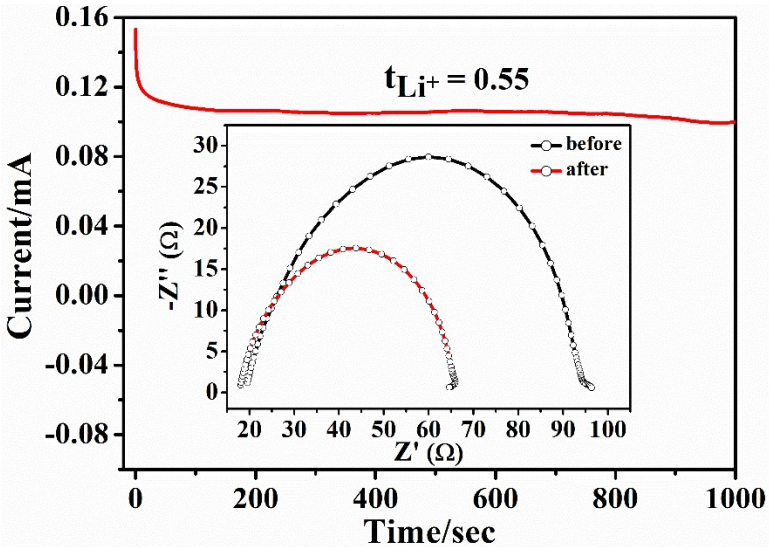

Figure S10. The current-time curve of solid-like electrolyte S-MIL-Cr during the polarization process (inside is the corresponding EIS before and after polarization).

Table S3. Summary of conductivity and transference number of different MOFs-based solid-state electrolytes.

NO.	Materials	σ (S cm^{-1})	t_{Li^+}	Ref
1	CSIL	2.1×10^{-3}	0.63	S8
2	ZIF-67@ZIF-8	1.35×10^{-3}	0.82	S6
3	**$LiNO_3$@HM-MIL**	**1.24×10^{-3}**	**0.86**	**This work**
4	LCMOF-1/PVDF-HFP/Li-IL	1.06×10^{-3}	0.36	S2
5	Zr-BPDC-2SO_3H	7.88×10^{-4}	0.88	S9
6	ZIF-8-SN-FEC	7.04×10^{-4}	0.68	S10
7	UiO-66-LiSS-50 wt% PC/EC	7.80×10^{-4}	0.88	S3
8	MIT-20-$LiBF_4$	4.8×10^{-4}	-	S11
9	MOF-688	3.4×10^{-4}	0.87	S4

10	UiO-66 (SLE-H)	3.3×10^{-4}	0.25	S12
11	$0.35LiO^{i}Pr + 0.25LiBF_4$	3.1×10^{-4}	-	S13
12	Li-IL@MOF	3.0×10^{-4}	0.36	S7
13	UiOLiTFSI	2.07×10^{-4}	0.84	S5
14	LGZ	1.61×10^{-4}	-	S1
15	PEO/ZIF-90-g-IL	1.17×10^{-4}	0.44	S14

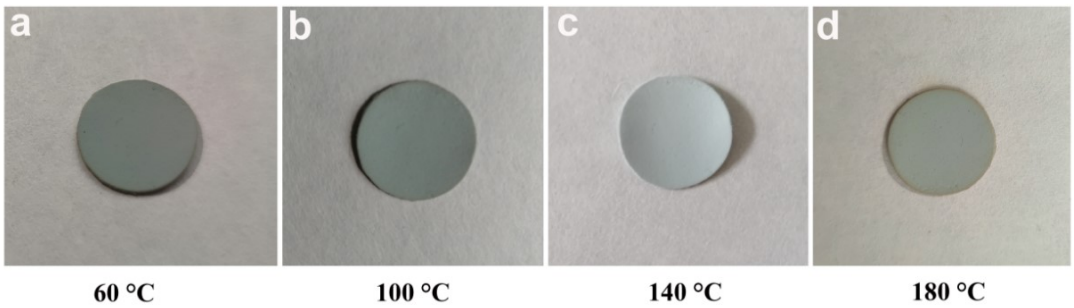

Figure S11. Photographs of $LiNO_3$@HM-MIL electrolyte membrane after 1 h storage at various temperature stages in an electric blow dryer atmosphere.

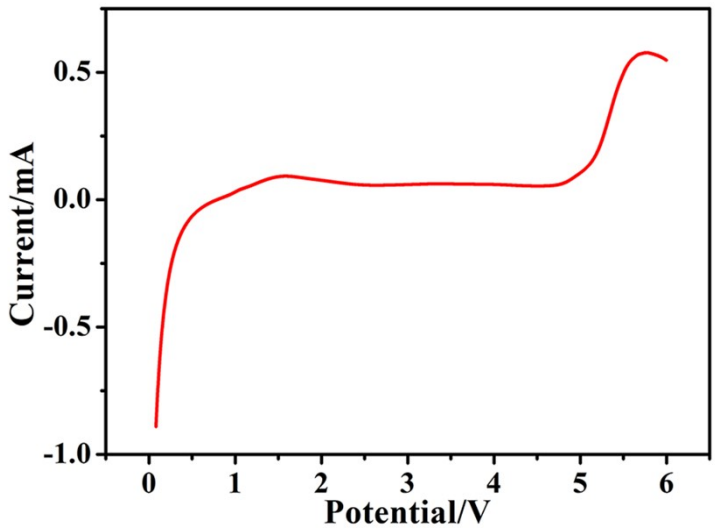

Figure S12. The LSV curves of SS|S-MIL-Cr electrolyte|Li battery.

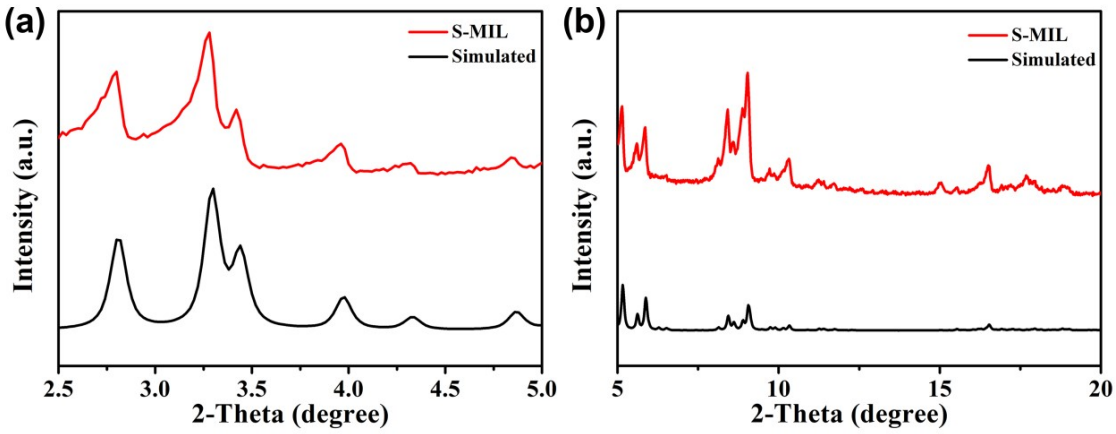

Figure S13. The PXRD patterns of the synthesized Al-doped solid bimetals S-MIL.

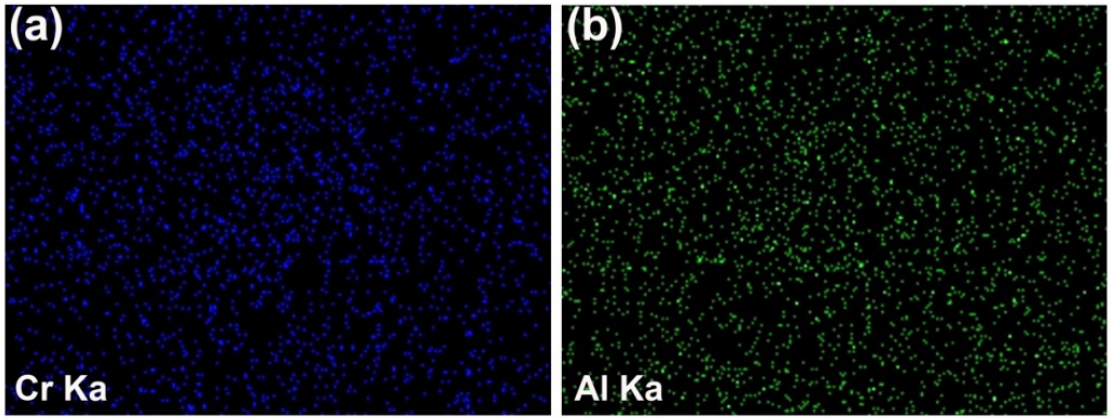

Figure S14. The SEM-EDX of the synthesized Al-doped solid bimetals S-MIL.

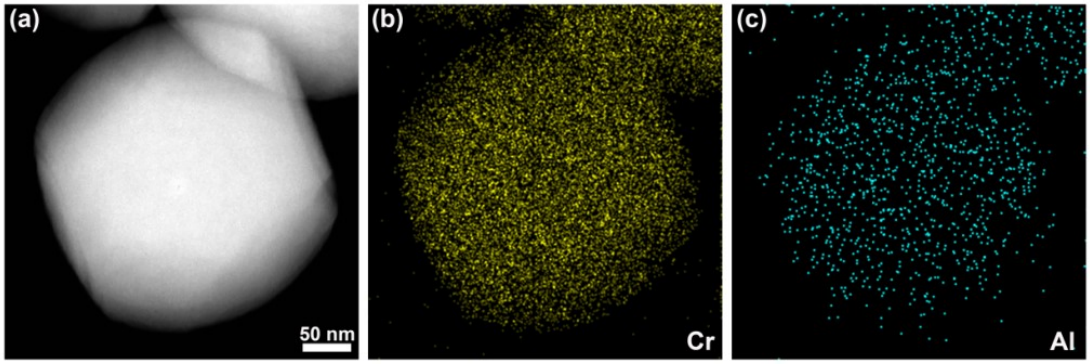

Figure S15. HAADF-STEM images of the synthesized Al-doped solid bimetals S-MIL (a) with the corresponding EDX elements mappings (b) and (c).

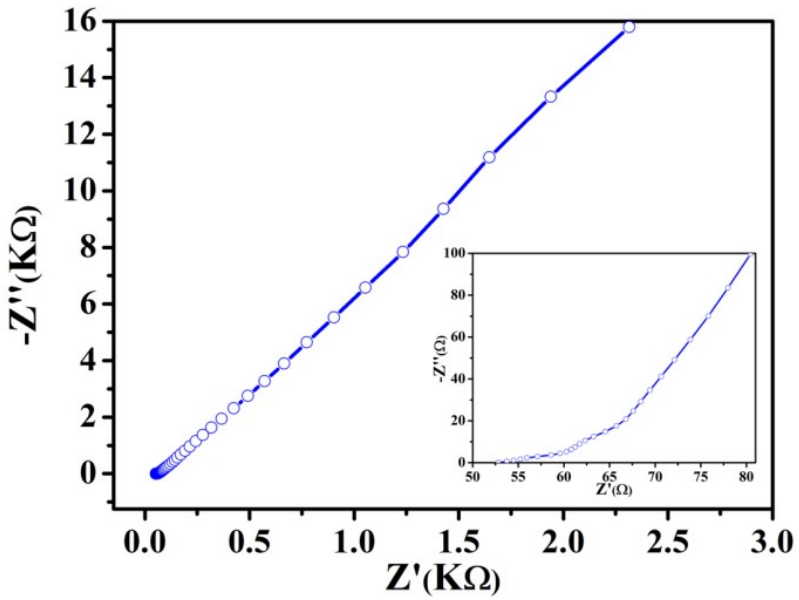

Figure S16. EIS of the synthesized Al-doped solid bimetals S-MIL at 25°C (the internal shows a magnified view of the high frequency area).

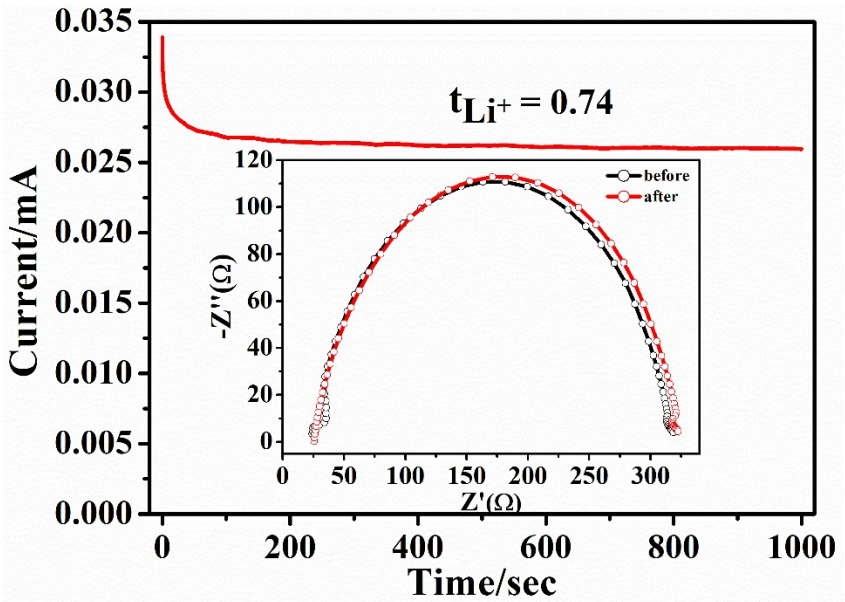

Figure S17. The current-time curve of the S-MIL solid-like electrolyte during the polarization process (inside is the corresponding EIS before and after polarization).

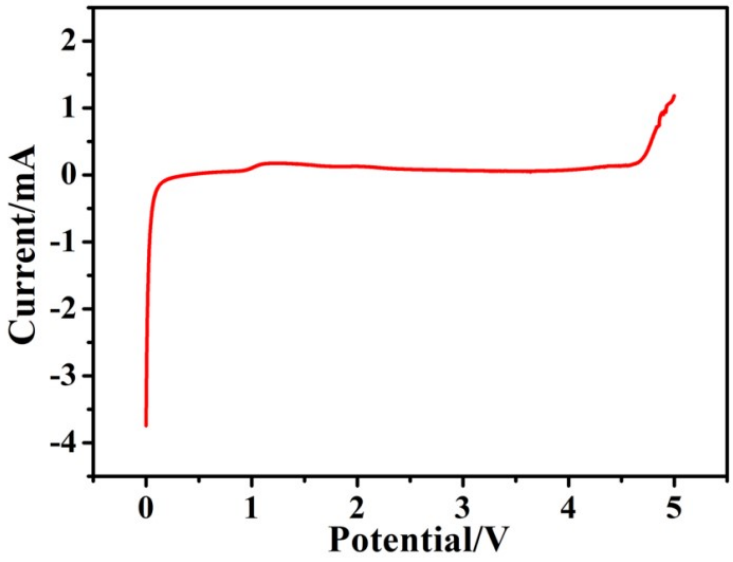

Figure S18. The LSV curves of SS|S-MIL solid-like electrolyte|Li battery.

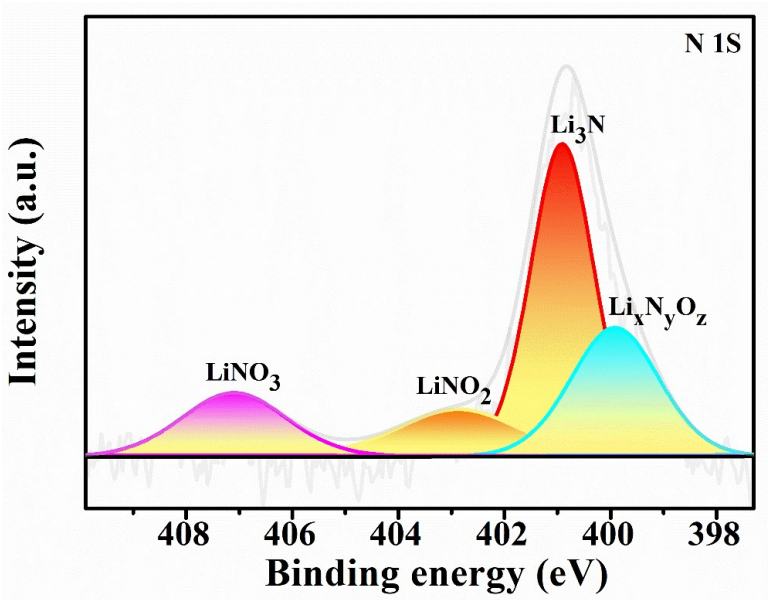

Figure S19. The XPS spectra of N 1s for $LiNO_3$@HM-MIL electrolyte after lithium plating/stripping cycles.

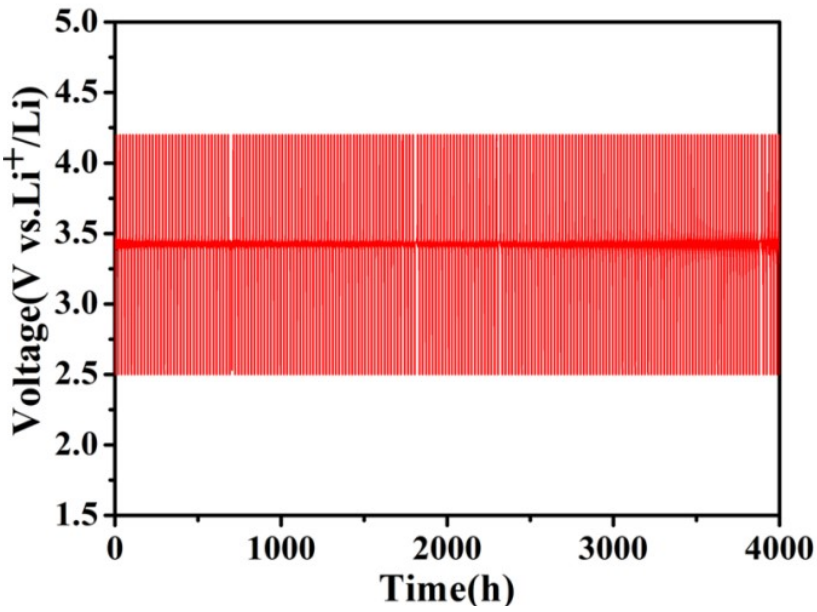

Figure S20. The galvanostatic charge and discharge cycling of $LiFePO_4$|$LiNO_3$@HM-MIL electrolyte|Li battery.

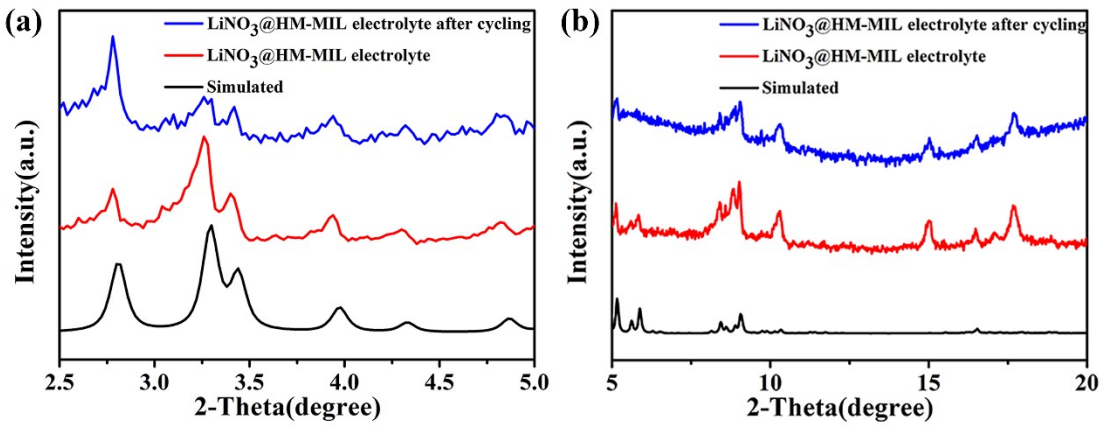

Figure S21. PXRD patterns of the hollow mesoporous $LiNO_3$@HM-MIL solid-like electrolyte before and after galvanostatic charge and discharge cycling.

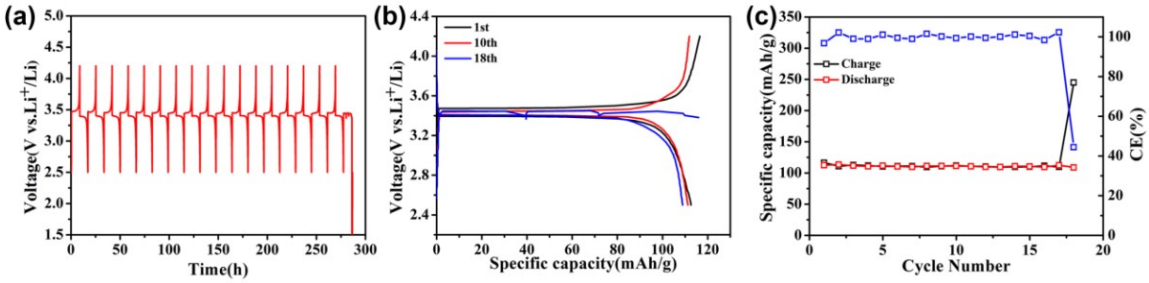

Figure S22. (a) The galvanostatic charge and discharge cycling of $LiFePO_4$|S-MIL-Cr electrolyte|Li battery; (b) The $LiFePO_4$|S-MIL-Cr electrolyte|Li battery charge and discharge curves for the 1st, 10nd and 18th cycles; (c) The charge/discharge capacity and coulombic efficiency of the $LiFePO_4$|S-MIL-Cr electrolyte|Li battery.

Table S4. Summary of cycle performance of different MOFs-based solid-state electrolytes.

NO.	Materials	current density	Initial discharge capacity/ mAh g^{-1}	After cycle discharge capacity/mA h g^{-1}	Capacity retention ratio/%	Ref
1	CSIL	0.2 C	-	158 (100 cycles)	99	S8
2	ZIF-67@ZIF-8	0.1 C	116	103.3 (100 cycles)	89.1	S6
3	UiO-66-LiSS-50wt%PC/EC	0.2 C	127	112 (100 cycles)	88.1	S3
4	LGZ	1.0 C	101.2	101.4 (500 cycles)	100	S1
5	Cu@Zn-MOF/PVA	1.0 C	119.3	135.3 (100 cycles)	-	S15
6	UiO-66 (SLE-H)	0.1 C	137	130 (100 cycles)	94.8	S12
7	Hollow ZIF-8	0.1 C	111.2	94.6 (100 cycles)	85.1	S16
8	PEO-n-UIO/60°C	0.1 C	151	141 (100 cycles)	95	S17
9	UIO/Li-IL/60°C	0.2 C	130.2	130.4 (100 cycles)	100	S18
		1.0 C	119	112 (380 cycles)	94	
10	MOF-688	30mA/g	125	120 (200 cycles)	96	S4
11	**$LiNO_3$@HM-MIL**	**0.1 C**	**131.96**	**128.56 (200 cycles)**	**97.42**	**This work**

References

1. G. Jiang, C. Qu, F. Xu, E. Zhang, Q. Lu, X. Cai, S. Hausdorf, H. Wang and S. Kaskel, *Adv. Funct. Mater.*, 2021, **31**, 2104300.
2. Q. Zhang, D. Li, J. Wang, S. Guo, W. Zhang, D. Chen, Q. Li, X. Rui, L. Gan and S. Huang, *Nanoscale*, 2020, **12**, 6976-6982.
3. H. Yang, B. Liu, J. Bright, S. Kasani, J. Yang, X. Zhang and N. Wu, *ACS Appl. Energy Mater.,* 2020, **3**, 4007-4013.
4. W. Xu, X. Pei, C. S. Diercks, H. Lyu, Z. Ji and O. M. Yaghi, *J. Am. Chem. Soc.*, 2019, **141**, 17522-17526.
5. F. Zhu, H. Bao, X. Wu, Y. Tao, C. Qin, Z. Su, Z. Kang, *ACS Appl. Mater. Interfaces,* 2019, **11**, 43206-43213.
6. Z. Liu, P. Liu, L. Tian, J. Xiao, R. Cui and Z. Liu, *Chem. Commun.*, 2020, **56**, 14629-14632.
7. Z. Wang, R. Tan, H. Wang, L. Yang, J. Hu, H. Chen and F. Pan, *Adv. Mater.*, 2018, **30**, 1704436.
8. A. E. Abdelmaoula, J. Shu, Y. Cheng, L. Xu, G. Zhang, Y. Xia, M. Tahir, P. Wu and L. Mai, *Small Methods*, 2021, **5**, 2100508.
9. Q. Zeng, J. Wang, X. Li, Y. Ouyang, W. He, D. Li, S. Guo, Y. Xiao, H. Deng, W. Gong, Q. Zhang and S. Huang, *ACS Energy Lett.*, 2021, **6**, 2434-2441.
10. D. Han, P. Wang, P. Li, J. Shi, J. Liu, P. Chen, L. Zhai, L. Mi and Y. Fu, *ACS Appl. Mater. Interfaces, 2*021, **13**, 52688-52696.
11. S. S. Park, Y. Tulchinsky and M. Dinca, *J. Am. Chem. Soc.*, 2017, **139**, 13260-13263.
12. K. Wang, L. Yang, Z. Wang, Y. Zhao, Z. Wang, L. Han, Y. Song and F. Pan, *Chem. Commun.*, 2018, **54**, 13060-13063.
13. B. M. Wiers, M. L. Foo, N. P. Balsara and J. R. Long, *J. Am. Chem. Soc.*, 2011, **133**, 14522-14525.
14. Z. Lei, J. Shen, J. Wang, Q. Qiu, G. Zhang, S. Chi, H. Xu, S. Li, W. Zhang, Y. Zhao, Y. Deng and C. Wang, *Chem. Eng. J.*, 2021, **412**, 128733.

15. L. Fan, Z. Guo, Y. Zhang, X. Wu, C. Zhao, X. Sun, G. Yang, Y. Feng and N. Zhang, *J. Mater. Chem. A*, 2020, **8**, 251-258.
16. L. Tian, Z. Liu, F. Tao, M. Liu and Z. Liu, *Dalton Trans.*, 2021, **50**, 13877-13882.
17. J. F. Wu and X. Guo, *J. Mater. Chem. A*, 2019, **7**, 2653-2659.
18. J. F. Wu and X. Guo, *Small*, 2019, **15**, 1804413.